JACS
JOURNAL OF THE AMERICAN CHEMICAL SOCIETY

ARTICLE

pubs.acs.org/JACS

A Reactive Ru−Binaphtholate Building Block with Self-Tuning Hapticity

Johanna M. Blacquiere, Carolyn S. Higman, Robert McDonald,[†] and Deryn E. Fogg*

Center for Catalysis Research & Innovation and Department of Chemistry, University of Ottawa, Ottawa, Ontario K1N 6N5, Canada

Supporting Information

ABSTRACT: A versatile Ru−BINO building block is reported, which offers a straightforward entry point into the chemistry of atropisomeric binaphtholate complexes of ruthenium. Reaction of $RuCl_2(PPh_3)_3$ **6a** with $Tl_2((S)\text{-BINO})$ affords $Ru((S)\text{-BINO})(PPh_3)_2$ **7** as a mixture of isomers: in **7′**, the BINO ligand is bound via η^3-*CCO*,η^1-*O′* donors, and in symmetrical **7″**, via η^3-*CCO*,η^3-*O′C′C′* interactions. The bis(enolate) BINO bonding mode in the latter, not previously observed for any metal, underscores the remarkable geometric and electronic flexibility of the binaphtholate moiety. The BINO ligand proves able to stabilize complexes containing as few as two, and as many as four, additional ligands in **7** and its derivatives, enabling a synthetic versatility that contrasts with that of the superficially similar *o*-catecholate complex $Ru(o\text{-cat})(PPh_3)_3$. As with the important achiral Ru precursor **6a**, complex **7** undergoes facile transformation into a range of products under mild conditions, including acetonitrile, pyridine, and vinylidene derivatives. Single-crystal X-ray structures are reported for three of these complexes: $Ru(\eta^3,\eta^3\text{-}(S)\text{-BINO})(PPh_3)_2$ **7″**, $Ru(\eta^3,\eta^1\text{-}(S)\text{-BINO})(PPh_3)_2(MeCN)$ **9**, and $Ru(\eta^3,\eta^1\text{-}(S)\text{-BINO})(PPh_3)(py)_2$ **11**. $^{13}C\{^1H\}$ NMR signatures are proposed for new and known BINO coordination modes (η^1-*O*,η^1-*O′*; η^1-*C1*,η^1-*O′*; η^3-*CCO*,η^3-*O′C′C′*; η^3-*CCO*,η^1-*O′*; η^6-C_6,η^1-*O′*), as a potential aid to further developments in late-metal BINO chemistry.

INTRODUCTION

The deployment of asymmetric catalysis in pharmaceutical and agrochemicals manufacturing[1,2] will undoubtedly see further expansion with massive projected increases in the global consumer population, coupled with increasing pressure on feedstocks. Among the "privileged" chiral auxiliaries[3] central to current asymmetric catalytic processes, the atropisomeric 1,1′-binaphthyl moiety stands out for its ubiquity and importance as a stereogenic element within both binaphtholates and their neutral derivatives (e.g., BINAP, the phosphoramidites, and MOP ligands). The parent 1,1′-binaphtholate (BINO) ligand and its 3,3′-functionalized derivatives have themselves been exploited in transformations ranging from conjugate addition, vinylation, and alkynylation of C═E functionalities (E = O, N) to Friedel−Crafts alkylation and hydroaminoalkylation, hydroamination/cyclization, and C−C coupling of olefins, including cycloaddition and olefin metathesis reactions.[4−6]

Prominent in much of this chemistry is the hard Lewis acid character of the catalysts, a reflection of the dominance of early and mid-transition elements, the lanthanides, and main group metals. Soft Lewis acids based on BINO complexes of the late transition metals have the potential to further expand this rich area of opportunity. Advances in group 10-BINO chemistry, particularly by the Gagné group, are notable in this context.[7,8] Despite the enormous scope of ruthenium catalysis,[9,10] however, Ru derivatives are very recent. The first example, 18-electron $Ru((R)\text{-BINO})(p\text{-cymene})$ **1**, was reported by Yao, Li, and coworkers in 2008,[11] while our group recently described Ru−BINO catalysts relevant to asymmetric olefin metathesis (**2**, **3**; Chart 1).[12] Both **1** and **2** exhibit multidentate chelation of the BINO ligand, in preference to the *O*,*O′*-binding prevalent in harder, more oxophilic metals (see also **4**, **5**; Chart 1).

The present work began with the search for a Ru−BINO building block that might retain the versatility of the important precursor complex $RuCl_2(PPh_3)_3$ **6a** (one of the most widely used starting materials in ruthenium chemistry)[13] within atropisomeric Ru−binaphtholate complexes. One aspect of this versatility arises from the capacity of **6a** to undergo *partial* functionalization or ligand exchange, with retention of a stabilizing phosphine group as required. An open question at the outset was whether reaction of **6a** with BINO would terminate at a very stable piano-stool complex, as found on treating $RuHCl(PPh_3)_3$ **6b** with the BINO derivative BINOP (see **5**, Chart 1),[14,15] or whether reactive, coordinatively unsaturated structures might be attainable. Here, we report the successful synthesis of $Ru((S)\text{-BINO})(PPh_3)_2$ **7**, as a mixture of isomers in which the BINO ligand is bound via oxygen and an η^3-*CCO* enolate moiety, or via a bis−enolate interaction; we describe the sensitive response of the BINO binding mode to the coordination environment at the metal, and the resulting capacity of **7** to support both exchange of the ancillary ligands and installation of additional reactive functionalities at the metal center.

RESULTS AND DISCUSSION

Installation of the BINO ligand on the ruthenium framework of **6a** proceeds in high yield at ambient temperature. Thus, addition of $Tl_2((S)\text{-BINO})$[16] to a purple suspension of **6a** in THF at 24 °C caused an immediate color change to pink and deposition of TlCl. Formation of $Ru((S)\text{-BINO})(PPh_3)_2$ **7** (Scheme 1a) was

Received: May 24, 2011
Published: August 15, 2011

Chart 1. Established Coordination Modes for Complexes of BINO and (See 5) BINOP[a]

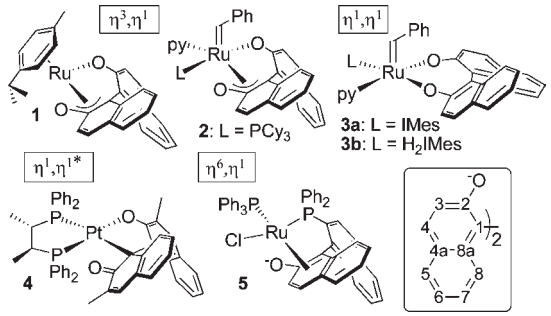

[a]BINOP = 1-diphenylphosphino-1,1′-binaphthyl-1′-olate; IMes = *N*, *N*′-bis(mesityl)imidazol-2-ylidene; py = pyridine. Numbering shown for one naphtholate ring; corresponding nuclei on the second bear a prime label. For simplicity, BINO binding is described in the text using the labels depicted. Thus, **2** is referred to as an η^3,η^1-BINO complex, rather than an η^3-*C,C,O*-BINO-κO structure. The asterisk in the label η^{1*} indicates the η^1-*C1* coordination mode in **4**.[7j]

Scheme 1. Reactions of 6a with (a) Binaphtholate and (b) *o*-Catecholate Ion

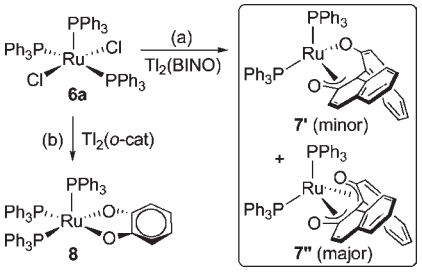

quantitative within 1 h: this product was isolated in 82% yield by filtration and reprecipitation from THF/hexanes. Charge-transfer MALDI-TOF MS[17] (Figure 1) and combustion analysis of **7** are consistent with the proposed formulation. In comparison, the corresponding reaction of **6a** with catecholate[18] terminates in tris-phosphine complex **8** (Scheme 1b). The difference in coordination mode and number is an early indicator of the structural and electronic versatility that proves a hallmark of the BINO ligand in this chemistry.

$^{31}P\{^1H\}$ NMR analysis of **7** reveals a 1:4 mixture of isomers in CD_2Cl_2 at room temperature (**7′**, 43.5 ppm; **7″**, 56.9 ppm; both singlets). Neither complex exhibits the extremes of BINO coordination seen in Chart 1: that is, binding through solely the oxygen sites (see **3**) or via an η^6-arene,η^1-*O*′ interaction analogous to the binding mode present in **5**.[19] Instead, we assign the minor, higher-field signal to isomer **7′**, containing an unsymmetrically η^3,η^1-bound BINO ligand, on the basis of its resolution into an AB pattern at slightly lower temperatures (15 °C: 43.7, 43.3 ppm; $^2J_{PP}$ = 19 Hz), as well as detailed $^{13}C\{^1H\}$ NMR analysis. NMR signatures associated with this and other BINO coordination modes are discussed in a subsequent section. The downfield singlet in the $^{31}P\{^1H\}$ NMR spectrum (the sole peak observed at 60 °C)[20] is due to complex **7″**, containing a novel, η^3,η^3-BINO binding mode: the nature of this interaction was confirmed by X-ray crystallographic (Figure 2a) and $^{13}C\{^1H\}$ NMR analysis. At 40 °C in C_6D_6,

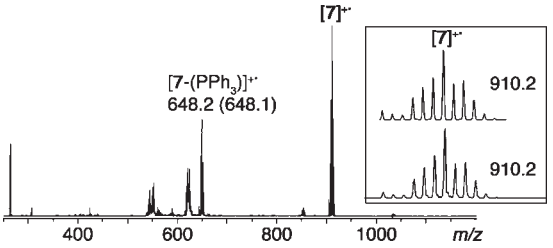

Figure 1. Charge-transfer MALDI mass spectrum of **7** (pyrene matrix). Inset: Simulated (top) and observed (bottom) isotope patterns.

interconversion occurs on the 2.2 s time-scale of the T_1 for **7′**, as indicated by spin saturation transfer experiments ($k_{exchange}$ = 0.29 s^{-1}), although a rigorously quantitative interpretation of the rate of chemical exchange is hampered by the potential for NOE effects.[21]

The parent systems **6** are classic ruthenium precursors for which phosphine dissociation gives entry to a rich catalytic and coordination chemistry,[13] including high-yield routes to catalytically important[9a,c,10] alkylidene, allenylidene, and vinylidene derivatives. The utility of the catecholate analogue Ru(η^1,η^1-*O*, *O*′-$O_2C_6H_4$)(PPh_3)$_3$ **8** (Scheme 1b) is limited in comparison, this complex resisting, for example, transformation into vinylidene or benzylidene derivatives.[18] To examine the influence of the BINO ligand on reactivity, we undertook treatment of **7** with acetonitrile and pyridine, as well as with *tert*-butylacetylene: the corresponding reactions of **6a** afford $RuCl_2(PPh_3)_2(L)_n$ derivatives (L = py, MeCN),[22] and vinylidene complex $RuCl_2(PPh_3)_2$-(=C=CH^{t}Bu),[23] respectively.

Acetonitrile Derivatives. Addition of neat MeCN to solid pink **7** resulted in immediate formation of an orange suspension, from which Ru(η^3,η^1-(*S*)-BINO)(PPh_3)$_2$(MeCN) **9** (Scheme 2a) was isolated as a dark pink solid in ca. 70% yield. Multinuclear NMR analysis in CD_2Cl_2 confirmed the presence of two, cis-disposed phosphine ligands (δ_P 49.1, 48.3 ppm; $^2J_{PP}$ = 22 Hz), and a single nitrile ligand (δ_C 120.3 ppm, δ_H 1.37 ppm). While X-ray analysis of crystals grown from THF−Et_2O suggests an η^2-interaction between the Ru center and the C2−O1 bond (Figure 2b), the 15 Hz magnitude of the C1−P coupling constant, as well as the ^{13}C NMR chemical shift data (vide infra), provide convincing evidence for an η^3,η^1-BINO structure in solution. The difference may reflect crystal packing effects.

Addition of CD_3CN to benzene solutions of **7** improves the solubility of the products and triggers coordination of a second acetonitrile ligand via slippage from η^3,η^1- to η^1,η^1-BINO binding. The equivalence of the PPh_3 ligands, which give rise to a well-resolved $^{31}P\{^1H\}$ NMR singlet at 45.5 ppm (1:2 CD_3CN−C_6D_6), is consistent with symmetrical Ru(η^1,η^1-(*S*)-BINO)-(PPh_3)$_2$(MeCN)$_2$ **10**. This is assigned as the sterically favored *trans*-PPh_3 isomer, given the absence of $^3J_{P-C2}$ coupling. Attempts to precipitate **10** yield only **9**, indicating facile exchange between these five- and six-coordinate species.

Pyridine Derivatives. Reaction of **7** with pyridine, in contrast, gives bis- and tris-pyridine derivatives Ru(η^3,η^1-(*S*)-BINO)(PPh_3)-(py)$_2$ **11** and Ru(η^1,η^1-(*S*)-BINO)(PPh_3)(py)$_3$ **12**, a reflection of the higher donor ability of this ligand, relative to acetonitrile (Gutmann donor number 33.1, vs 14.1 kcal mol^{-1}).[24] In neat pyridine-d_5, **7** is rapidly and completely converted into orange **12** (Scheme 2b), the $^{31}P\{^1H\}$ NMR singlet for the latter (56.0 ppm) integrating 1:1 versus free PPh_3. Only minor amounts of **12** were isolated, however, when the pyridine solution was stripped of solvent, subjected to azeotropic removal of free pyridine with hexanes, and

dx.doi.org/10.1021/ja204767a |*J. Am. Chem. Soc.* 2011, 133, 14054–14062

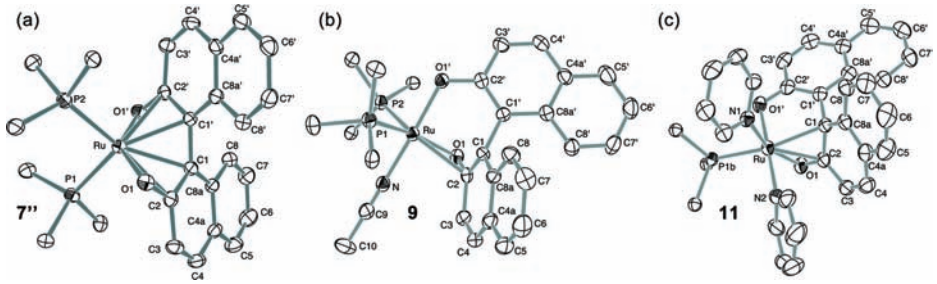

Figure 2. Perspective views of (a) Ru(η^3,η^3-(*S*)-BINO)$(PPh_3)_2$ **7″**, (b) Ru(η^3,η^1-(*S*)-BINO)$(PPh_3)_2$(MeCN) **9**, and (c) Ru(η^3,η^1-(*S*)-BINO)-$(PPh_3)(py)_2$ **11**, showing the labeling scheme for key atoms. Non-hydrogen atoms are represented by Gaussian ellipsoids at the 50% probability level. For clarity, hydrogen atoms are not shown, solvate molecules present for **9**·THF and **11**·Et_2O·0.25THF are omitted, and phosphine phenyl groups are truncated to the ipso-carbons.

Scheme 2. Reactions of 7 with (a) Acetonitrile, (b) Pyridine, and (c) *tert*-Butylacetylene[a]

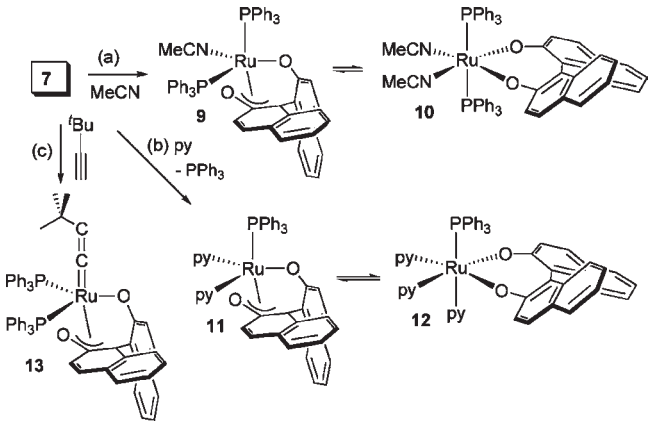

[a] For clarity, exchange reactions between η^3 and η^1 sites in **11** (see text) are omitted.

treated with pentane to precipitate the product. The resulting fine orange suspension consisted principally of **11** (ca. 20% **12** present; 76% total yield). The proportion of **12** decreases further on washing the filtrand with pentane.

Solutions of the initially obtained crude product in CD_2Cl_2 exhibit a broad $^{31}P\{^1H\}$ NMR singlet due to **11**, accompanied by a sharp singlet for **12** (58.3 and 56.1 ppm, respectively; 20% **12**). The breadth of the signal for **11** we attribute to dynamic averaging between η^3-enolate and η^1-*O* sites at room temperature, a process observed previously with **1**,[11] and proposed for **4**.[7j] At −20 °C, the peak sharpens ($\omega_{1/2}$ diminishes from 45 to 5 Hz), and the corresponding $^{13}C\{^1H\}$ NMR spectrum suggests an η^3,η^1-BINO structure, in which the PPh_3 ligand lies trans to C1, as judged from the large P−C coupling constant of 19 Hz. Such a bonding mode is indeed evident on X-ray analysis of crystals of **11** that deposited from THF−Et_2O (Figure 2c). On cooling the NMR sample further, to −40 °C, a new $^{31}P\{^1H\}$ NMR singlet emerges at 48.3 ppm (ca. 20% of total integration): this may plausibly be due to the reduced-hapticity isomer Ru-(η^1,η^1-(*S*)-BINO)$(PPh_3)(py)_2$, but $^{13}C\{^1H\}$ NMR confirmation is precluded by the relatively low abundance of this species.

Vinylidene Derivative. A final experiment was directed at examining the ease of converting **7** into a vinylidene complex. Reaction of **6a** with *tert*-butylacetylene affords $RuCl_2(PPh_3)_2$-(=C=CH^{t}Bu),[23] as noted above, while catecholate complex **8** proved inert to such treatment.[18] Complex **7**, in comparison, underwent an immediate color change from red to dark purple, with quantitative conversion to Ru(η^3,η^1-(*S*)-BINO)$(PPh_3)_2$-(=C=CH^{t}Bu) (**13**; Scheme 2c). The product was isolated by precipitation from THF−hexanes, albeit in only 40% yield, due to its high solubility. The structure depicted in Scheme 2c is supported by NMR, IR, and combustion analysis. Retention of two inequivalent phosphine ligands is evident from the AB pattern in the $^{31}P\{^1H\}$ NMR spectrum (64.4, 38.3 ppm; $^2J_{PP}$ = 27 Hz), while the vinylidene ligand gives rise to a strong, diagnostic infrared ν(C=C) band at 1633 cm^{-1}, as well as the expected NMR correlations between the C*H* multiplet at 3.08 ppm and the Ru=*C* and $C(CH_3)_3$ signals at 347.2 and 0.72 ppm, respectively ($^1H-^{13}C$ HMBC; $^1H-^1H$ COSY). A dynamic process operative at room temperature obscures the ^{13}C NMR signals above 135 ppm, and hence unequivocal assignment of the coordination mode, as this is the region occupied by the critical C2/C2′ signals. Low-temperature analysis is consistent with an η^3,η^1-BINO coordination mode (see next section), albeit with significant electronic perturbation at C1, relative to other such complexes.[25] Complex **13** differs from the other examples studied in containing a strongly π-acidic vinylidene ligand, as discussed below.

NMR Signatures for BINO Coordination Modes. BINO, like its important derivative BINAP and related ligands,[26] is evidently characterized by great flexibility and variety in its coordination to late-metal centers. To facilitate future development, we sought to establish NMR markers for the different BINO coordination modes. As the NMR values for the key ^{13}C nuclei have not been routinely reported, the chemical shift ranges proposed below must be regarded as preliminary: whether they indeed correlate directly with coordination mode will become clearer as the number of crystallographically and spectroscopically characterized examples expands, but such a correlation would greatly aid in structural assignment where X-ray analysis is inconvenient or infeasible. In general most sensitive to changes in naphtholate binding are the chemical shifts of C2/C2′ and C1/C1′ (Figure 3a).[27] The former appear generally more diagnostic, as discussed below. $^{13}C\{^1H\}$ NMR signals for these ipso carbons were most readily located via ^1H-detected HMBC experiments; a "road map" for assignment of these and the remaining BINO carbons is given in the Supporting Information.

For η^1-*O*,η^1-*O*′-BINO complexes (e.g., **3a**, **3b**, **10**, **12**; Table 1), the aryloxy carbons C2 and C2′ appear at ca. 168 ppm, and C1/C1′ at ca. 126 ppm. These locations appear relatively insensitive to changes in the NMR solvent (Table 2). For the η^3-*CCO*, η^1-*O*′-BINO complexes (e.g., **1**, **2**, **7′**, **9**, **11**), the chemical shift for C2′ in the

dx.doi.org/10.1021/ja204767a |*J. Am. Chem. Soc.* 2011, 133, 14054–14062

η^1-bound ring shows minimal change, appearing at ca. 172 ppm. That for C1′ moves 10 ppm upfield, however (to ca. 115 ppm), a reflection of the sensitivity of C1′ to the enolate environment at the immediately adjacent C1 nucleus. The η^3-*CCO* carbons themselves can exhibit more dramatic upfield shifts, depending on the extent of shielding by the electrons circulating in the enolate π-system: an average value of 148 ppm is seen for C2 and 97 ppm for C1. Variable back-donation results in a rather broad range of values for C2 (±6 ppm) and, especially, C1 (±12 ppm), as shown in blue and red, respectively, in Figure 3a. Omitted from these ranges are the values for **13**, which is anomalous within this series in containing a highly π-acidic vinylidene ligand (a π-acceptor comparable to CO).[28] This is expected to limit shielding of the η^3-enolate nuclei: indeed the signal for C1 appears at ca. 126 ppm, a location typical for η^1-bound BINO, although C2 is less affected.

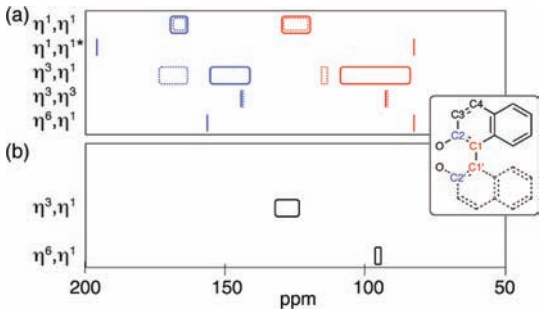

Figure 3. ^{13}C NMR signatures for different BINO coordination modes. (a) Chemical shift ranges for C2/C2′ (blue) and of C1/C1′ (red), as in Table 1; dashed lines correspond to the "prime" nuclei.[27] The asterisk in the label η^{1*} indicates the η^1-*C1* coordination mode in **4**.[7g,j] (b) Supplementary chemical shifts of C3/C4 (black), where assignment on the basis of (a) alone is ambiguous.

Within the ranges indicated for the more typical η^3-enolates appear the corresponding signals for both naphtholate rings of the η^3,η^3-BINO complex **7″** (C2/C2′, 145 ppm; C1/C1′, 93 ppm).[29] For phosphine derivatives, $^3J_{CP}$ splitting of the C1/C1′ signal(s) is valuable in confirming the presence of a direct Ru−C1 interaction, although the dependence on the dihedral angle means that negative evidence is less reliable.

The rarer η^1-*C1*,η^1-*O*′ coordination mode exhibits a diagnostic ketone signal for C2 (196 ppm for complex **4**),[7g,j] although the 82 ppm location for C1 is not far from the lower end of the range for η^3,η^1-BINO complexes. Finally (and in contrast to the examples above, all of which can be assigned from the combined C1/C1′ and C2/C2′ chemical shifts), the η^6,η^1-binding mode in complex **5** is distinguishable from η^3,η^1-BINO binding only once a ca. 30 ppm upfield shift[14] for both C3 and C4 is also taken into consideration, as illustrated in Figure 3b.

CONCLUSION

The BINO ligand offers a powerful source of chirality that has been exploited with great success in asymmetric catalysis by hard Lewis acid−base complexes. Its incorporation into soft late-metal complexes, a challenge of sustained interest, is here expanded to a versatile ruthenium−binaphtholate building block. The remarkable geometric and electronic flexibility of the binaphtholate ligand is demonstrated by its capacity to coordinate in modes ranging from η^1-*O*,η^1-*O*′ to η^1-*O*,η^3-*C*′*C*′*O*′ and, in the extreme, η^3-*CCO*, η^3-*C*′*C*′*O*′ binding, in addition to others previously established. ^{13}C{^{1}H} NMR signatures for each binding mode are suggested on the basis of current data, as an aid to structural assignment; the small sample sets, however (particularly for the singular η^3, η^3-BINO complex **7″**), means that the proposed correlations of BINO coordination modes with chemical shift ranges should be

Table 1. ^{13}C{^{1}H} NMR Ranges Associated with Different BINO or (for 5) BINOP Coordination Modes (See Also Figure 3)[a,27]

entry	coord. mode	compd	C1	C2	C1′	C2′	ref
1	η^1,η^1	**3a**, **3b**, **10**, **12**	126 ± 2	168 ± 4	126 ± 2	169 ± 1	Table 2
2	η^3,η^1	**1**, **2**, **7′**, **9**, **11**	97 ± 12	148 ± 6	115 ± 2	172 ± 2	Table 2
3	η^3,η^3	**7″**	93.2 (t, $^2J_{CP}$ = 4 Hz)	144.7	93.2 (t, $^2J_{CP}$ = 4 Hz)	144.7	this work
4	η^6,η^1	**5**[b]	83.0	155.6	–[c]	–[c]	14
5	η^1,η^{1*}	**4**	82.4	195.5 (d, 6 Hz)	–[c]	–[c]	7g,7j

[a] Values at ambient temperature, except **11**−**12** (20% **12**; 253 K, CD_2Cl_2); **13** (213 K); **1** (210 K). Values for **7″**, **5**, **4** in CD_2Cl_2; for others, see Table 2. Values for vinylidene complex **13** are anomalous (see text) and are omitted. Peaks are singlet multiplicity, unless otherwise specified. (*) indicates the η^1-*C1* coordination mode in **4**. [b] Ranges for C3/C4: 95−97 ppm, versus 124−135 for these resonances in η^3,η^1-BINO complexes. [c] Assignment not reported.

Table 2. ^{13}C{^{1}H} NMR Data for Individual Compounds Grouped into Entries 1 and 2 of Table 1[a]

coord. mode	compd	solvent	C1	C2	C1′	C2′	ref
η^1,η^1	**3a**	CD_2Cl_2	124.2	164.0	123.9	170.1	12
	3b	CD_2Cl_2	123.9	164.0	123.9	170.3	12
	10	$CD_3CN-C_6D_6$ (1:2)	127.4	168.9	127.4	168.9	*b*
	12	C_5D_5N	128.1	171.0	127.8	169.7	*b*
	12	CD_2Cl_2	not located	169.8	not located	168.7	*b*
η^3,η^1	**1**	CD_2Cl_2	85.0	141.5	114.0	170.9	11
	2	CD_2Cl_2	95.6 (d, $^2J_{CP}$ = 11 Hz)	154.1 (d, $^2J_{CP}$ = 3 Hz)	116.8	174.1 (d, $^3J_{CP}$ = 5 Hz)	12
	7′	CD_2Cl_2	109.1 (d, $^2J_{CP}$ = 16 Hz)	143.1	114.2 (d, $^3J_{CP}$ = 2 Hz)	170.4 (d, $^3J_{CP}$ = 5 Hz)	*b*
	9	CD_2Cl_2	106.4 (d, $^2J_{CP}$ = 15 Hz)	143.3 (d, $^2J_{CP}$ = 2 Hz)	115.2 (d, $^3J_{CP}$ = 1 Hz)	172.1 (d, $^3J_{CP}$ = 5 Hz)	*b*
	11	CD_2Cl_2	97.6 (d, $^2J_{CP}$ = 19 Hz)	143.5	113.8	174.4 (d, $^3J_{CP}$ = 5 Hz)	*b*
	13	CD_2Cl_2	125.6 (t, $^2J_{CP}$ = 4 Hz)	148.0 (t, $^2J_{CP}$ = 4 Hz)	116.0	162.0	*b*

[a] For conditions, see footnote to Table 1. [b] This work.

regarded as preliminary. Importantly, these BINO enolates are labile; η^3-coordination provides a source of coordinative stabilization where required, but does not impede binding of additional ligands at the metal center. Complexes containing as few as two, and as many as four, additional ligands are thus accessible. The chemistry of Ru(BINO)$(PPh_3)_2$ **7** described above aligns well with that of the important, achiral ruthenium precursor $RuCl_2(PPh_3)_3$ **6a**, and compares favorably with the more circumscribed scope of its close relative Ru(*o*-cat)$(PPh_3)_3$. Complex **7** thus offers a potentially powerful and convenient entry point into the chemistry of atropisomeric binaphtholate complexes of ruthenium.

EXPERIMENTAL SECTION

General. Reactions were carried out at room temperature (24 °C) under N_2 using standard Schlenk or glovebox techniques. Dry, oxygen-free solvents were obtained using a Glass Contour solvent purification system and were stored over Linde 4 Å molecular sieves. Pyridine was distilled over sodium benzophenone ketyl and was stored over activated sieves (Linde 4 Å) in an amber bottle in the glovebox. $CDCl_3$ was distilled over CaH_2 and stored over activated sieves (Linde 4 Å). 1, 1′-Binaphthol ((*S*)-BINOL; 99% optical purity; Strem) and pyrene, anhydrous CD_2Cl_2, and pyridine-d_5 (all Aldrich) were used as received. $RuCl_2(PPh_3)_3$[30] was prepared by literature methods. NMR spectra were recorded on Bruker Avance 300 and Avance 500 spectrometers, at 296 K unless otherwise specified. Chemical shifts are reported relative to TMS (^{13}C, ^1H) or 85% external H_3PO_4 (^{31}P) at 0 ppm and were referenced to the carbon or residual proton signal of the deuterated solvent. Microanalyses were carried out by Guelph Chemical Laboratories (Guelph, ON) and X-ray analyses by Dr. Robert McDonald of the University of Alberta X-ray Crystallography Laboratory. Charge-transfer (CT) MALDI-TOF mass spectra were collected using a Bruker Daltonics Omniflex MALDI-TOF mass spectrometer coupled to an MBraun glovebox, as previously described.[17]

Synthesis of Tl_2((*S*)-BINO). Addition of (*S*)-BINOL (862 mg, 3.01 mmol) to a stirred solution of TlOEt (1.652 g, 6.628 mmol) in Et_2O (10 mL) afforded a pale yellow precipitate. The suspension was stirred at room temperature for 15 h, after which the solid was isolated by filtration and washing with Et_2O (2 mL). Yield 87%. Caution: Tl salts are toxic[31] and must be handled using appropriate protection and secondary containment; wastes and contaminated material must be disposed of in accordance with federal regulations.

Synthesis of Ru((*S*)-BINO)$(PPh_3)_2$ 7. A suspension of Tl_2 ((*S*)-BINO) (326 mg, 0.470 mmol) and $RuCl_2(PPh_3)_3$ **6a** (450 mg, 0.470 mmol) in 12 mL of THF was stirred for 1 h at 24 °C, over which time it turned from purple to pink. $^{31}P\{^1H\}$ NMR analysis indicated complete reaction. As the suspension was too fine to filter off, the solvent was stripped off under vacuum. The residue was taken up in benzene, filtered through Celite, then glass-fiber filter paper, and the Ru product was washed through with benzene. The filtrate was stripped to dryness to give a dark residue, which was redissolved in THF (ca. 0.5 mL), treated with hexanes (6 mL), and chilled to −35 °C. The air-sensitive red-pink product was filtered off, washed with cold hexanes (3 mL) and cold 3:1 hexanes−Et_2O (3 × 1 mL), and then dried. Yield: 351 mg (82%). CT-MALDI MS (pyrene matrix), *m*/*z*: $[7]^{+\bullet}$ 910.2 (simulated: 910.2). Anal. Calcd for $C_{56}H_{42}O_2P_2Ru$: C, 73.92; H, 4.65. Found: C, 74.23; H, 4.38. The product contained a mixture of 7″ and 7′ (ratio 4:1 in CD_2Cl_2), the spectroscopic data for which are separated for convenience below. X-ray quality crystals of 7″ deposited from THF by vapor diffusion of hexanes at 24 °C. NMR signatures for the novel η^3, η^3-BINO coordination mode in 7″ were established from $^1H-^{13}C$ HMBC spectra measured at 60 °C, to suppress signals for 7′. (Both isomers are generally present, including at −80°C in C_7D_8; solely 7″ is observed in $CDCl_3$, but decomposition over the time-scale required for 2D NMR analysis prevents characterization in this solvent.) Signals for 7′ were assigned by spectral subtraction of resonances for 7″ from the room-temperature spectrum of the two isomers in CD_2Cl_2. For the BINO numbering scheme, see Chart 1. The majority of the BINO signals in these, as well as the other new complexes, could be assigned using the roadmap provided in the Supporting Information.[32]

Ru(η^3,η^3-(*S*)-BINO)$(PPh_3)_2$ 7″. $^{31}P\{^1H\}$ NMR (121.4 MHz, CD_2Cl_2): δ 56.9 (s), 56.5 ppm in $CDCl_3$. ^1H NMR (CD_2Cl_2, 500.1 MHz): δ 7.38 (m, 4H, *H5* and *H6*), 7.34 (d, $^3J_{H4H3}$ = 9.3 Hz, 2H, *H4*), 7.26 (m, 2H, *H7*), 7.22−7.06 (m, 10H, *Ar*), 6.91 (overlap; 28H, *Ar*; includes *H8* of 7″ and *H3*′, *H6*′ of 7′), 6.44 (d, $^3J_{H3H4}$ = 9.3 Hz, 2H, *H3*). ^{13}C NMR (CD_2Cl_2, 125.6 MHz): δ 144.7 (s, C2), 137.8 (s, *C8a*), 137.4 (s, *C4*), 134.6 (d, J_{CP} = 10 Hz, *Ph*), 134.1 (br, *Ph*), 133.8 (d, J_{CP} = 10 Hz, *Ph*), 132.3 (d, J_{CP} = 10 Hz, *Ph*), 132.2 (d, J_{CP} = 4 Hz, *Ph*), 130.9 (s, *C4a*), 130.2 (d, J_{CP} = 1 Hz, *Ph*), 129.4 (s, *C5*), 129.2 (br, *Ph*), 128.1 (d, J_{CP} = 6 Hz, *Ph*), 128.0 (d, J_{CP} = 6 Hz, *Ph*), 127.4 (s, *C7*), 127.3 (m, *Ph*), 124.9 (s, *C8*), 124.5 (s, *C6*), 124.3 (s, *C3*), 93.2 (t, $^2J_{C1P}$ = 4 Hz, *C1*).

Ru(η^3,η^1-(*S*)-BINO)$(PPh_3)_2$ 7′ (20%). Chemical shifts are given for key peaks only; extraction of most multiplicities and integration values was hampered by overlap with the signals due to the major product 7″. $^{31}P\{^1H\}$ NMR (121.4 MHz, CD_2Cl_2): 43.5 (s). At 288 K: 43.7 (d, $^2J_{PP}$ = 19.4 Hz), 43.3 (d, $^2J_{PP}$ = 19.4 Hz). ^1H NMR (CD_2Cl_2, 500.1 MHz): δ 8.17 (d, $^3J_{H4H3}$ = 9 Hz, *H4*), 7.89 (d, $^3J_{H5H6}$ = 8 Hz, *H5*), 7.55 (*H5*′), 7.29 (*H3*), 7.45 (*H4*′), 7.27 (*H6*), 6.88 (*H3*′), 6.86 (*H6*′), 6.70 (*H7* and *H7*′), 6.57 (*H8*), 5.96 (d, $^3J_{H8'H7'}$ = 9 Hz, *H8*′). ^{13}C NMR (CD_2Cl_2, 125.6 MHz): 170.4 (d, $^3J_{CP}$ = 5 Hz, *C2*′), 143.1 (s, C2), 141.3 (d, $^3J_{CP}$ = 3 Hz, *C8a*), 135.1 (s, *C4*), 133.4 (s, *C8a*′), 129.6 (s, *C8*), 128.9 (s, *C4*′), 128.8 (s, *C4a*), 128.6 (s, *C5*), 128.2 (s, *C5*′), 127.4 (s, *C7*), 127.2 (s, *C4a*′), 124.9 (s, *C7*′), 124.6 (s, *C6*), 124.4 (s, *C3*), 124.2 (s, *C8*′), 123.9 (s, *C3*′), 119.8 (s, *C6*′), 114.2 (d, $^3J_{CP}$ = 2 Hz, *C1*′), 109.1 (d, $^3J_{CP}$ = 16 Hz, *C1*).

Synthesis of Ru(η^3,η^1-(*S*)-BINO)$(PPh_3)_2$(MeCN) 9. Addition of acetonitrile (0.5 mL) to solid 7 (151 mg, 0.166 mmol) resulted in an immediate color change from pink to orange, and complete conversion to **9** ($^{31}P\{^1H\}$ NMR analysis). The suspension was stirred for 5 min, then stripped of solvent, treated with cold hexanes (2 mL), and chilled to −35 °C. The fine solid was isolated by pipetting off the supernatant and was dried under vacuum. Yield: 120.5 mg (76%). Anal. Calcd for $C_{58}H_{45}NO_2P_2Ru$: C, 73.25; H, 4.77; N, 1.47. Found: C, 72.97; H, 4.61; N, 1.20. Single crystals of **9**·THF deposited from THF by vapor diffusion of diethyl ether (Et_2O) at 24 °C. NMR analysis in CD_2Cl_2 revealed only signals for **9**. $^{31}P\{^1H\}$ NMR (CD_2Cl_2, 121.4 MHz): δ 49.1 (d, $^2J_{PP}$ = 22 Hz), 48.3 (d, $^2J_{PP}$ = 22 Hz). ^1H NMR (CD_2Cl_2, 500.1 MHz): δ 8.00 (d, $^3J_{H4H3}$ = 9.5 Hz, 1H, *H4*), 7.81 (d, $^3J_{H5H6}$ = 7.5 Hz, 1H, *H5*), 7.57−7.51 (m, 8H, *H5*′ and *Ph*), 7.40 (d, $^3J_{H4'H3'}$ = 8.5 Hz, 1H, *H4*′), 7.28−7.25 (m, 3H, *Ar*), 7.19 (d, $^3J_{H3H4}$ = 9.0 Hz, 1H, *H3*), 7.17 (m, 1H, *H6*), 7.14−7.11 (m, 10H, *Ph*), 6.92−6.89 (m, 7H, *H3*′ and *Ph*), 6.80 (m, 1H, *H6*′), 6.66 (m, 1H, *H7*′), 6.62 (m, 1H, *H7*), 6.58 (d, $^3J_{H8H7}$ = 5.0 Hz, 1H, *H8*), 6.55−6.51 (m, 6H, *Ph*), 5.91 (d, $^3J_{H8'H7'}$ = 8.5 Hz, 1H, *H8*′), 1.37 (s, 3H, CH_3CN). ^{13}C NMR (CD_2Cl_2, 125.6 MHz): δ 172.1 (d, J_{CP} = 5 Hz, *C2*′), 143.3 (d, J_{CP} = 2 Hz, *C2*), 142.3 (d, J_{CP} = 2 Hz, *C8a*), 134.8 (s, *C8a*′), 134.65 (d, J_{CP} = 8.8 Hz, *Ph*), 133.8 (d, J_{CP} = 10.0 Hz, *Ph*), 133.1 (s, *C4*), 129.9 (s, *C3*), 129.4 (s, *C8*), 128.8 (s, *C4a*), 128.7 (s, *C4*′), 128.3 (s, *C5*), 127.9 (m, *C5*′ and *Ph*), 126.9 (s, *C7*), 126.8 (s, *C4a*′), 124.6 (s, *C7*′), 124.5 (s, *C3*′), 123.9 (s, *C8*′), 123.3 (s, *C6*), 120.3 (s, CH_3CN), 118.9 (s, *C6*′), 115.2 (d, $^2J_{CP}$ = 1 Hz, *C1*′), 106.4 (d, $^2J_{CP}$ = 15 Hz, *C1*), 3.41 (s, CH_3CN). IR (Nujol): ν(C≡N) 2263 cm^{-1} (w).

In probe reactions, **7** (ca. 10 mg) was dissolved in 1:2 CD_3CN:C_6D_6 and analyzed ($^{31}P\{^1H\}$ NMR). Solely bis-nitrile, η^1,η^1-BINO complex **10** was observed; at lower proportions of CD_3CN, signals for **9** emerged. Poor solubility precluded analysis in neat CD_3CN.

Ru(η^1,η^1-(*S*)-BINO)$(PPh_3)_2$(MeCN)$_2$ 10. $^{31}P\{^1H\}$ NMR (1:2 CD_3CN:C_6D_6, 121.4 MHz): δ 45.5 (s). ^1H NMR (1:2 CD_3CN:C_6D_6, 500.1 MHz): 7.56 (d, $^3J_{H5H6}$ = 8 Hz, 2H, *H5*), 7.45−7.35 (m, 13H, *Ph*),

Table 3. Crystallographic Collection Parameters for 7″, 9·THF, and 11·Et_2O·0.25THF

	7″	9·THF	11·Et_2O·0.25THF
CCDC no.	796872	796870	796871
empirical formula	$C_{56}H_{42}O_2P_2Ru$	$C_{62}H_{53}NO_3P_2Ru$	$C_{53}H_{49}N_2O_{3.25}PRu$
color, shape	red, prism	orange, plate	orange, prism
formula weight	909.91	1023.06	897.98
temp (K)	173(2)	173(2)	173(2)
wavelength (Å)	0.71073	0.71073	0.71073
crystal system	orthorhombic	orthorhombic	orthorhombic
space group	$P2_12_12_1$ (No. 19)	$P2_12_12_1$ (No. 19)	$P2_12_12$ (No. 18)
crystal size (mm)	0.14 × 0.13 × 0.10	0.44 × 0.11 × 0.03	0.43 × 0.25 × 0.24
a (Å)	13.0968 (6)	13.1015 (5)	18.0557 (4)
b (Å)	14.0641 (7)	13.4592 (5)	19.4773 (5)
c (Å)	23.0032 (11)	28.5044 (10)	12.7568 (3)
α (deg)	90	90	90
β (deg)	90	90	90
γ (deg)	90	90	90
V (Å^3)	4237.1 (4)	5026.3 (3)	4486.26 (19)
Z, calcd density (g/cm^3)	4, 1.426	4, 1.352	4, 1.330
μ (mm^{-1})	0.490	0.424	0.431
F(000)	1872	2120	1864
θ range for data collectn	2.29° < θ < 24.94°	1.43° < θ < 25.69°	1.54° < θ < 27.51°
limiting indices	$-16 \le h \le 16$	$-15 \le h \le 15$	$-23 \le h \le 23$
	$-17 \le k \le 17$	$-16 \le k \le 16$	$-25 \le k \le 25$
	$-28 \le l \le 28$	$-34 \le l \le 34$	$-16 \le l \le 16$
reflections collected/unique	34 014/8676 (R_{int} = 0.0496)	37 705/9548 (R_{int} = 0.0785)	40 159/10 315 (R_{int} = 0.0195)
absorption correction	Gaussian integration (face-indexed)		
max, min transmission	0.9535−0.9323	0.9891−0.8355	0.9044−0.8377
structure solution method	Patterson/structure expansion (DIRDIF-2008)	Patterson/structure expansion (DIRDIF-2008)	direct methods (SHELXS-97)
data/restraints/params	8676/0/550	9548/10/611	10 315/3/528
GOF (S)[a]	1.027	1.023	1.083
final R indices	R_1 = 0.0268	R_1 = 0.0380	R_1 = 0.0316
R_1[b] [$F_o^2 \ge 2\sigma(F_o^2)$] wR_2 (all data)	wR_2 = 0.0561	wR_2 = 0.0812	wR_2 = 0.0985
largest diff peak and hole (e Å^{-3})	0.328 and −0.316	0.650 and −0.392	1.028 and −0.358

[a] $S = [\Sigma w(F_o^2 - F_c^2)^2/(n-p)]^{1/2}$ (n = number of data; p = number of parameters varied; $w = [\sigma^2(F_o^2) + (0.0232P)^2 + 0.7848P]^{-1}$, where $P = [\max(F_o^2, 0) + 2F_c^2]/3$). [b] $R_1 = \Sigma||F_o| - |F_c||/\Sigma|F_o|$; w$R_2 = [\Sigma w(F_o^2 - F_c^2)^2/\Sigma w(F_o^4)]^{1/2}$.

7.20 (d, $^3J_{H4H3}$ = 9 Hz, 2H, *H4*), 7.1−6.85 (m, 30H, *Ar*; includes *H8* at 7.00 (d, $^3J_{H8H7}$ = 8 Hz)), 6.79 (m, 2H, *H7*), 6.71 (m, 2H, *H6*), 6.12 (d, $^3J_{H3H4}$ = 9 Hz, 2H, *H3*), 1.35 (m, 3H, CH_3CN). $^{13}C\{^1H\}$ NMR (1:2 CD_3CN:C_6D_6, 125.6 MHz): δ 168.9 (s, *C2*), 135.9 (s, *C8a*), 134.7 (m, *Ph*), 129.1 (s, *C3*), 128.4−127.6 (overlap of residual C_6D_5H, *Ph*, BINO: within this range, *C4a* (128.3) and *C5* (127.6) located by correlation experiments), 127.4 (s, *C1*), 126.8 (s), 125.4 (s, *C8*), 125.0 (br s, *C4*), 123.9 (s, *C7*), 119.3 (s, *C6*), 116.9 (s, CH_3CN), 0.3 (s, CH_3CN).

Synthesis of Ru(η^3,η^1-(*S*)-BINO)(PPh_3)(py)$_2$ 11 and Ru-(η^1,η^1-(*S*)-BINO)(PPh_3)(py)$_3$ 12. Addition of 0.5 mL of pyridine to **7** (93.2 mg, 0.102 mmol) caused an immediate color change from red to orange. NMR analysis indicated complete conversion to **12**. Vacuum removal of pyridine afforded a gel, to which hexanes (1 mL) were added with stirring, then pumped off to effect azeotropic removal of pyridine (3×). Addition of pentane (1 mL) then gave a fine suspension. A bright orange solid was filtered off and washed with cold pentane (62 mg, 76%). $^{31}P\{^1H\}$ NMR analysis revealed **11** and **12** (ratio 4:1; the proportion of **12** decreases with further washing). The spectroscopic data are separated for convenience below. X-ray quality crystals of **11**·Et_2O·0.25 THF deposited from THF by vapor diffusion of Et_2O at 24 °C; combustion analysis was carried out on the crushed and dried crystals. Anal. Calcd for $C_{48}H_{37}N_2O_2$-PRu: C, 71.54; H, 4.63; N, 3.48. Found: C, 71.26; H, 4.37; N, 3.15.

Ru(η^3,η^1-(*S*)-BINO)(PPh_3)(py)$_2$ 11 (Diagnostic ^{31}P and ^{1}H NMR Signals). $^{31}P\{^1H\}$ NMR (CH_2Cl_2 + 20 μL of C_6D_6 for lock, 121.4 MHz, 296 K): δ 58.3 (br s). ^{1}H NMR (CD_2Cl_2, 500.1 MHz, 253 K): δ 8.93 (d, $^3J_{HH}$ = 5 Hz, 1H, py H_o), 8.75 (d, $^3J_{HH}$ = 6 Hz, 1H, py), 8.58−8.57 (m, 3H, py), 8.15 (d, $^3J_{HH}$ = 5 Hz, 1H, py), 7.55−7.47 (overlapping m, 10H, *Ar*; includes *H5′*, *H7*), 7.41 (d, $^3J_{HH}$ = 8 Hz, 1H, *H4′*), 7.04−7.00 (overlapping m, 1.5H, *Ar*; includes *H4*), 6.94−6.80 (overlapping m, 5H, *Ar*; includes *H3′*, *H6′*), 6.74−6.65 (overlapping m, 2H, *Ar*; includes *H7′*), 6.09 (d, $^3J_{H3H4}$ = 9 Hz, 1H, *H3*), 5.91 (br d, $^3J_{H8'H7'}$ = 9 Hz, 1H, *H8′*), 5.62 (d, *J* = 5 Hz, 1H, *Ar*).

Ru(η^1,η^1-(*S*)-BINO)(PPh_3)(py)$_3$ 12 (20%). Only key peaks are identified; extraction of multiplicities and integration values was hampered by overlap with signals for the major product **11**. $^{31}P\{^1H\}$ NMR (CH_2Cl_2 + 20 μL of C_6D_6 for lock, 121.4 MHz, 296 K): δ 56.1 (s). ^{1}H NMR (CD_2Cl_2, 500.1 MHz, 296 K): 6.97 (*H4*), 6.91 (*H4′*).

Combined $^{13}C\{^1H\}$ NMR signals for the **11**−**12** mixture (CD_2Cl_2, 125.6 MHz, 253 K): δ 174.4 (d, $^3J_{CP}$ = 5 Hz, *C2′*, **11**), 169.7 (s, *C2*, **12**),

168.1 (s, *C2′*,**12**), 158.4 (s), 158.0 (s), 157.1 (s), 155.8 (s), 154.7 (br s), 152.8 (s), 149.9 (s), 143.5 (s, *C2*, **11**), 142.0 (s, *C8a*, **11**), 137.2 (s), 136.0 (s), 135.7 (s), 135.2 (s, *C8a′*, **11**), 135.0 (s), 134.8 (s), 134.4 (d, J_{CP} = 9 Hz), 134.2−134.1 (m), 133.9 (s), 133.7 (d, J_{CP} = 19 Hz), 133.5 (s), 133.4 (s, *C4*, **11**), 133.1 (s), 133.0 (s), 132.1 (s), 132.0 (s), 132.0 (s), 131.9 (s), 129.2 (s), 128.9 (s), 128.6 (d, J_{CP} = 7 Hz), 128.0−127.9 (m, includes *C4′* and *C5*, **11**), 127.8 (s), 127.7 (s, *C5′*, **11**), 127.6 (s), 127.4 (s), 127.2 (s), 126.8 (s, *C4a*, **11**), 126.7 (s), 126.69 (s), 126.6 (s), 126.5 (s), 125.9 (s), 125.4 (s, *C3*, **11**), 125.3 (s), 124.7 (s, *C7′*, **11**), 124.3 (d, J_{CP} = 2 Hz, *C3′*, **11**), 124.2 (s), 123.8 (s), 123.7 (s), 123.6 (s), 123.5 (s), 123.1 (s), 123.0 (s), 122.6 (s, *C8′*, **11**), 122.2 (br s), 119.3 (s), 119.1 (s), 118.7 (s, *C6′*, **11**), 113.8 (s, *C1′*, **11**), 97.6 (d, $^2J_{CP}$ = 19 Hz, *C1*, **11**).

In Situ Formation of 12 in Pyridine-d_5. $^{31}P\{^1H\}$ NMR (C_6D_5N, 121.4 MHz): δ 57.3 (s). ^1H NMR (C_6D_5N, 500.1 MHz): δ 7.78−7.68 (m), 7.58 (br s), 7.50−7.42 (m), 7.38−7.34 (m, *Ar*; includes *H4*), 7.31−7.25 (m, *Ar*; includes *H4′*), 7.22 (br s), 7.20−7.04 (m), 6.97−6.83 (m, *Ar*; includes *H3* and *H3′*). $^{13}C\{^1H\}$ NMR (C_5D_5N, 125.6 MHz): δ 171.0 (s, *C2*), 169.7 (s, *C2′*), 137.9 (s), 137.8 (s), 136.9 (s), 136.3 (s), 136.0 (s), 135.9 (s), 135.1 (s), 134.9 (s), 134.8 (s), 134.2 (s), 134.1 (s), 132.4 (s), 132.3 (s), 132.2 (s), 132.16 (s), 129.2 (s), 129.1 (s), 129.0 (s), 129.01 (s), 128.9 (s), 128.42−128.35 (m), 128.2 (s), 128.1 (s, *C1*), 128.06 (s), 127.94−127.90 (m), 127.8 (s, *C1′*), 127.6 (s), 127.5 (s, *C3′*), 127.1 (s), 126.1 (s), 126.0 (s), 125.8 (s), 125.6 (s), 124.1 (s), 123.9 (s), 123.8−123.3 (solvent signals overlap; *C3* located (123.5) by correlation experiments), 123.1 (s), 119.8 (s), 119.5 (s).

Synthesis of Ru(η^3,η^1-(*S*)-BINO)(PPh_3)$_2$(=C=CH^{t}Bu) 13. Slow, dropwise addition of *tert*-butylacetylene (0.08 mL of a 16.6% *v*/*v* solution in C_6H_6; 2 equiv) to **7** (46.5 mg, 0.051 mmol) in 1 mL of C_6H_6 caused an immediate color change from red to purple. The reaction was stirred for 5 min, then stripped, dissolved in THF (0.3 mL), and treated with hexanes (4 mL) and cooled to −35 °C. The purple precipitate was filtered off, washed with cold hexanes, and dried. Yield: 23 mg (45%). Anal. Calcd for $C_{62}H_{52}O_2P_2Ru$: C, 75.06; H, 5.28. Found: C, 75.08; H, 5.41. $^{31}P\{^1H\}$ NMR (121.4 MHz, CD_2Cl_2): δ 64.4 ($^2J_{PP}$ = 27 Hz), 38.3 ($^2J_{PP}$ = 27 Hz). ^1H NMR (CD_2Cl_2, 500.1 MHz, 213 K): δ 8.53 (d, $^3J_{H3H4}$ = 9 Hz, 1H, *H3*), 8.01 (d, $^3J_{H4H3}$ = 9 Hz, 1H, *H4*), 7.90 (d, $^3J_{H5H6}$ = 8 Hz, 1H, *H5*), 7.66 (d, $^3J_{H5′H6′}$ = 8 Hz, 1H, *H5′*), 7.56 (d, $^3J_{H4′H3′}$ = 9 Hz, 1H, *H4′*), 7.45−7.30 (m, 12H, *H6* and *Ph*), 7.12 (m, 10H, *Ph*), 7.00 (m, 5H, *H6′*, *H7*, *H8* and *H8′*), 6.91 (m, 3H, *H7′*), 6.84 (m, 7H, *H3′* and *Ph*), 3.08 (br s, 1H, CC*H*^{t}Bu), 0.72 (s, 9H, C(CH_3)$_3$). ^{13}C NMR (CD_2Cl_2, 125.6 MHz, 213 K): δ 347.2 (unresolved, Ru=*C*=CHC(CH_3)$_3$), 162.0 (s, *C2′*), 148.0 (unresolved m, *C2*), 135.3 (s, *C8a*), 134.0−133.0 (overlap; *Ph* and *C8a′*), 132.7 (s, *Ph*), 132.3 (s, *Ph*), 130.8 (s, *C3*), 130.2 (s, *Ph*), 128.8 (s, *C4a*), 128.1 (s, *Ph*), 127.9 (s, *C4*), 127.8−127.1 (overlap; *C8*, *C8′*, *C5*, *C5′* and *Ph*), 126.6 (m, *C4′*), 126.1 (s, *C4a′*), 125.6 (t, J_{CP} = 4 Hz, *C1*), 125.0 (s, *C7*), 124.3 (s, *C7′*), 123.6 (s, *C3′*), 122.8 (s, *C6*), 121.1 (s, Ru=C=CHC-(CH_3)$_3$), 119.8 (s, *C6′*), 116.0 (s, *C1′*), 67.6 (s, Ru=C=CH*C*(CH_3)$_3$), 30.9 (s, Ru=C=CHC(CH_3)$_3$). IR (Nujol): ν(C=C) 1633 cm^{-1} (m).

Spin Saturation Transfer Measurement. Complex **7** (10 mg) was dissolved in C_6D_6 in an NMR tube. At 40 °C, the $^{31}P\{1H\}$ NMR signal for **7″** (57.5 ppm) was saturated by irradiation, and the decrease in intensity of **7′** (40.0 ppm) was measured. The T_1 relaxation time for **7′** (at 2.2 s) was established using the inversion−recovery method and analyzing with the spectrometer T_1 routine.

Crystallography. Single crystals of **7″**, **9**·THF, and **11**·Et_2O·0.25 THF were analyzed using a Bruker D8/APEX II CCD diffractometer, with graphite-monochromated Mo K_a radiation at 173 K. Programs for diffractometer operation, data collection, data reduction, and absorption correction were those supplied by Bruker. Details of data collection, solution, and refinement are given in Table 3. The structures were solved using Patterson/structure expansion (DIRDIF-2008;[33] for **7″**, **9**) or SHELXS-97 (**11**) and were refined using full-matrix least-squares on F^2 in SHELXL-97.[34] For **9**·THF, O−C distances within the disordered THF solvate were constrained to be equal (within 0.03 Å) to a common refined value, as were the C−C distances. For **11**·Et_2O·0.25 THF, distances within the THF solvate were restrained to idealized values during refinement: *d*(O10S−C11S) = 1.46(1) Å; *d*(C11S−C12S) = *d*(C12S−C12S′) = 1.52(1) Å (C12S′ is related to C12S via the crystallographic 2-fold rotational axis (0, 1/2, *z*), upon which O10S is located). CCDC 796872 (**7″**), 796870 (**9**), and 796871 (**11**) contain the supplementary crystallographic data for this Article. These can be obtained free of charge from the Cambridge Crystallographic Data Centre via www.ccdc.cam.ac.uk/data_request/cif.

■ ASSOCIATED CONTENT

Supporting Information. Details of the approach used to assign $^{13}C\{^1H\}$ NMR signals for C1/C1′ and C2/C2′ of the BINO ligand; NMR spectra, including VT and spin saturation experiments; and crystallographic information files (CIF). This material is available free of charge via the Internet at http://pubs.acs.org.

■ AUTHOR INFORMATION

Corresponding Author
dfogg@uottawa.ca

Present Addresses
[†]X-ray Crystallography Laboratory, Chemistry Department, University of Alberta, 11227 Saskatchewan Drive NW, Edmonton, AB T6G 2G2, Canada.

■ ACKNOWLEDGMENT

This work was funded by NSERC of Canada. NSERC is thanked for a CGS-D award to J.M.B. and a CGS-M award to C.S.H.

■ REFERENCES

(1) Blaser, H.-U., Federsel, H.-J., Eds. *Asymmetric Catalysis on Industrial Scale*, 2nd ed.; Wiley-VCH: Weinheim, 2010.

(2) Blaser, H.-U.; Hoge, G.; Pugin, B.; Spindler, F. Industrial Applications of Homogeneous Enantioselective Catalysts. In *Handbook of Green Chemistry*; Anastas, P. T., Crabtree, R. H., Eds.; Wiley-VCH: Weinheim, 2009; Vol. 1, pp 153−203.

(3) Yoon, T. P.; Jacobsen, E. N. *Science* **2003**, *299*, 1691–1693.

(4) For selected reviews of catalysis via complexes of BINO or 3,3′-derivatized BINO derivatives, see: (a) Najera, C.; Sansano, J. M.; Sa, J. M. *Eur. J. Org. Chem.* **2009**, 2385–2400. (b) Brunel, J. M. *Chem. Rev.* **2007**, *107*, PR1–PR45. (c) Brunel, J. M. *Chem. Rev.* **2005**, *105*, 857–897. (d) Shibasaki, M.; Matsunaga, S. *J. Organomet. Chem.* **2006**, *691*, 2089–2100. (e) Chen, Y.; Yekta, S.; Yudin, A. K. *Chem. Rev.* **2003**, *103*, 3155–3211.

(5) Selected recent examples or reviews of C=E bond elaborations catalyzed by BINO complexes (and, in some cases, organocatalysts). Conjugate addition: (a) Koripelly, G.; Rosiak, A.; Rossle, M. *Synthesis* **2007**, *9*, 1279–1300. Alkynylation or vinylation:(b) Tanaka, K.; Kukita, K.; Ichibakase, T.; Kotani, S.; Nakajima, M. *Chem. Commun.* **2011**, *47*, 5614–5616. (c) Huang, G.; Yang, J.; Zhang, X. *Chem. Commun.* **2011**, *47*, 5587–5589. (d) Blay, G.; Cardona, L.; Climent, E.; Pedro, J. R. *Angew. Chem., Int. Ed.* **2008**, *47*, 5593–5596. Other nucleophilic additions:(e) DeBerardinis, A. M.; Turlington, M.; Pu, L. *Angew. Chem., Int. Ed.* **2011**, *50*, 2368–2370. (f) Kaur, P.; Pindi, S.; Wever, W.; Rajale, T.; Li, G. *Chem. Commun.* **2010**, *46*, 4330–4332. (g) Yukawa, T.; Seelig, B.; Xu, Y.; Morimoto, H.; Matsunaga, S.; Berkessel, A.; Shibasaki, M. *J. Am. Chem. Soc.* **2010**, *132*, 11988–11992. (h) Hatano, M.; Horibe, T.; Ishihara, K. *J. Am. Chem. Soc.* **2010**, *132*, 56–57. (i) Liu, W.-J.; Lv, B.-D.; Gong, L.-Z. *Angew. Chem., Int. Ed.* **2009**, *48*, 6503–6506. (j) Sone, T.; Lu, G.; Matsunaga, S.; Shibasaki, M. *Angew. Chem., Int. Ed.* **2009**, *48*, 1677–1680. (k) Muramatsu, Y.; Harada, T. *Angew. Chem., Int. Ed.* **2008**, *47*, 1088–1090.

(6) Selected examples or reviews of recent BINO complex-catalyzed C═C bond elaborations. Friedel−Crafts alkylations: (a) Bandini, M.; Umani-Ronchi, A. *Catalytic Asymmetric Friedel-Crafts Alkylations*; Wiley-VCH: Weinheim, 2009. Olefin hydroaminoalkylation or hydroamination/cyclization: (b) Reznichenko, A. L.; Emge, T. J.; Audorsch, S.; Klauber, E. G.; Hultzsch, K. C.; Schmidt, B. *Organometallics* **2011**, *30*, 921–924. (c) Gribkov, D. V.; Hultzsch, K. C.; Hampel, F. *J. Am. Chem. Soc.* **2006**, *128*, 3748–3759. Cycloaddition:(d) Repka, L. M.; Ni, J.; Reisman, S. E. *J. Am. Chem. Soc.* **2010**, *132*, 14418–14420. (e) Yan, P.; Jing, H. *Adv. Synth. Catal.* **2009**, *351*, 1325–1332. (f) Ward, D. E.; Shen, J. *Org. Lett.* **2007**, *9*, 2843–2846. Olefin metathesis:(g) Sattely, E. S.; Meek, S. J.; Malcolmson, S. J.; Schrock, R. R.; Hoveyda, A. H. *J. Am. Chem. Soc.* **2009**, *131*, 943–953.

(7) For Pt−BINO complexes, see: (a) Peng, H.-Y.; Lam, C.-K.; Mak, T. C. W.; Cai, Z.; Ma, W.-T.; Li, Y.-X.; Wong, H. N. C. *J. Am. Chem. Soc.* **2005**, *127*, 9603–9611. (b) Voshell, S. M.; Gagné, M. R. *Organometallics* **2005**, *24*, 6338–6350. (c) Ait-Haddou, H.; Leeder, S. M.; Gagné, M. R. *Inorg. Chim. Acta* **2004**, *357*, 3854–3864. (d) Doherty, S.; Newman, C. R.; Rath, R. K.; van den Berg, J.-A.; Hardacre, C.; Nieuwenhuyzen, M.; Knight, J. G. *Organometallics* **2004**, *23*, 1055–1064. (e) Doherty, S.; Newman, C. R.; Rath, R. K.; Luo, H.-K.; Nieuwenhuyzen, M.; Knight, J. G. *Org. Lett.* **2003**, *5*, 3863–3866. (f) Becker, J. J.; Gagné, M. R. *Organometallics* **2003**, *22*, 4984–4998. (g) Brunkan, N. M.; Gagné, M. R. *Organometallics* **2002**, *21*, 4711–4717. (h) Becker, J. J.; White, P. S.; Gagné, M. R. *J. Am. Chem. Soc.* **2001**, *123*, 9478–9479. (i) Tudor, M. D.; Becker, J. J.; White, P. S.; Gagné, M. R. *Organometallics* **2000**, *19*, 4376–4384. (j) Brunkan, N. M.; White, P. S.; Gagné, M. R. *J. Am. Chem. Soc.* **1998**, *120*, 11002–11003. (k) Brunkan, N. M.; White, P. S.; Gagné, M. R. *Angew. Chem., Int. Ed.* **1998**, *37*, 1579–1582. For Pd derivatives, see (c), (e), and:(l) Pelz, K. A.; White, P. S.; Gagné, M. R. *Organometallics* **2004**, *23*, 3210–3217. (m) Bergens, S. H.; Leung, P. H.; Bosnich, B.; Rheingold, A. L. *Organometallics* **1990**, *9*, 2406–2408.

(8) A few group 9 BINO complexes have also been reported. See: Paisner, S. N.; Lavoie, G. G.; Bergman, R. G. *Inorg. Chim. Acta* **2002**, *334*, 253–275 and ref 11, which describes Ir and Rh derivatives, as well as the first Ru example.

(9) Selected reviews: (a) Delaude, L.; Demonceau, A. NHC-Iron, Ruthenium and Osmium Complexes in Catalysis. In *N-Heterocyclic Carbenes*; Diez-Gonzalez, S., Ed.; RSC: Oxford, 2011; Vol. 6, pp 196−227. (b) Mezzetti, A. *Dalton Trans.* **2010**, *39*, 7851–7869. (c) Odedra, A.; Liu, R.-S. Ruthenium Vinylidenes in the Catalysis of Carbocyclization. In *Metal Vinylidenes and Allenylidenes in Catalysis*; Bruneau, C., Dixneuf, P. H., Eds.; Wiley-VCH: Weinheim, 2008; pp 193−216. (d) Morris, R. H. Ruthenium and Osmium. In *Handbook of Homogeneous Hydrogenation*; de Vries, J. G., Elsevier, C. J., Eds.; Wiley-VCH: Weinheim, 2007; Vol. 1, pp 45−70. (e) Faller, J.; Parr, J. *Curr. Org. Chem.* **2006**, *10*, 151–163. (f) Bruneau, C.; Derien, S.; Dixneuf, P. H. *Top. Organomet. Chem.* **2006**, *19*, 295–326. (g) Trost, B. M.; Frederiksen, M. U.; Rudd, M. T. *Angew. Chem., Int. Ed.* **2005**, *44*, 6630–6666. (h) Naota, T.; Takaya, H.; Murahashi, S.-I. *Chem. Rev.* **1998**, *98*, 2599–2660.

(10) Selected recent reviews of Ru-catalyzed olefin metathesis: (a) Vougioukalakis, G. C.; Grubbs, R. H. *Chem. Rev.* **2010**, *110*, 1746–1787. (b) Lozano-Vila, A. M.; Monsaert, S.; Bajek, A.; Verpoort, F. *Chem. Rev.* **2010**, *110*, 4865–4909. (c) Monfette, S.; Fogg, D. E. *Chem. Rev.* **2009**, *109*, 3783–3816. (d) Samojlowicz, C.; Bieniek, M.; Grela, K. *Chem. Rev.* **2009**, *109*, 3708–3742. (e) Malacea, R.; Dixneuf, P. H. Ruthenium Allenylidenes and Indenylidenes as Catalysts in Alkene Metathesis. In *Metal Vinylidenes and Allenylidenes in Catalysis*; Bruneau, C., Dixneuf, P. H., Eds.; Wiley-VCH: Weinheim, 2008; pp 251−277.

(11) Panichakul, D.; Su, Y.; Li, Y.; Deng, W.; Zhao, J.; Li, X. *Organometallics* **2008**, *27*, 6390–6392.

(12) Blacquiere, J. M.; McDonald, R.; Fogg, D. E. *Angew. Chem., Int. Ed.* **2010**, *49*, 3807–3810.

(13) Seddon, E. A.; Seddon, K. R. *The Chemistry of Ruthenium*; Elsevier: Amsterdam, 1984.

(14) Snelgrove, J. L.; Conrad, J. C.; Moriarty, M. M.; Yap, G. P. A.; Fogg, D. E. *Organometallics* **2005**, *24*, 103–109.

(15) Related η^6- and η^5-ArO structures form on treating **6a**, **6b**, and other labile Ru precursors with aryloxide salts. See, for example: (a) Chaudret, B. N.; Cole-Hamilton, D. J.; Nohr, R. S.; Wilkinson, G. *J. Chem. Soc., Dalton Trans.* **1977**, 1546–1557. (b) Cole-Hamilton, D. J.; Young, R. J.; Wilkinson, G. *J. Chem. Soc., Dalton Trans.* **1976**, 1995–2001. (c) Christ, M. L.; Sabo-Etienne, S.; Chung, G.; Chaudret, B. *Inorg. Chem.* **1994**, *33*, 5316–5319. (d) Snelgrove, J. L.; Conrad, J. C.; Yap, G. P. A.; Fogg, D. E. *Inorg. Chim. Acta* **2003**, *345*, 268–278. (e) Abdur-Rashid, K.; Fedorkiw, T.; Lough, A. J.; Morris, R. H. *Organometallics* **2004**, *23*, 86–94.

(16) Use of the less toxic K_2(BINO) gave impure products and was therefore not pursued.

(17) Eelman, M. D.; Blacquiere, J. M.; Moriarty, M. M.; Fogg, D. E. *Angew. Chem., Int. Ed.* **2008**, *47*, 303–306. *Angew. Chem.* **2008**, *120*, 309–312.

(18) Monfette, S.; Duarte Silva, J. A.; Gorelsky, S. I.; Dalgarno, S. J.; dos Santos, E. N.; Araujo, M. H.; Fogg, D. E. *Can. J. Chem.* **2009**, *87*, 361–367.

(19) We originally described the binding of the "aryloxy" ring in **5** as η^5-C_5 (ref 14); such a structure was crystallographically established for the related phenoxide complex RuH(η^5-C_6H_5O)(PPh_3)$_2$, among others (refs 15d,15e). Compilation of the $^{13}C\{^1H\}$ NMR chemical shift data for this and other complexes in the present work revealed that the values for **5** are in fact consistent with η^6-coordination of the naphtholate ring.

(20) Cf. 1:1 **7′**:**7″** at −80 °C in C_7D_8. Attempts to extract activation parameters from a van't Hoff analysis were hindered by emergence of a further, unidentified process. The position of the **7′**−**7″** equilibrium is also strongly solvent-dependent; see the Supporting Information for details.

(21) Mann, B. E. *J. Magn. Reson.* **1976**, *21*, 17–23.

(22) (a) Wilkinson, G.; Gilbert, J. D. *J. Chem. Soc. A* **1969**, 1749–1753. (b) Wilkinson, G.; Cole-Hamilton, D. J. *J. Chem. Soc., Dalton Trans.* **1979**, 1283–1289.

(23) Wakatsuki, Y.; Yamazaki, H.; Kumegawa, N.; Satoh, T.; Satoh, J. Y. *J. Am. Chem. Soc.* **1991**, *113*, 9604–9610.

(24) Gutmann, V. *Coord. Chem. Rev.* **1976**, *18*, 225–255.

(25) The chemical shifts observed on cooling to −60 °C (C1, 125.6; C2, 148.0; C1′, 116.0; C2′, 162.0 ppm; cf., ranges shown in Figure 3a) are consistent with η^3,η^1-coordination of the BINO ligand in **13**, with the exception of the signal for C1. The latter is ca. 30 ppm downfield of the average room-temperature value exhibited by other such complexes; see Table 1. The difference may reflect reduced backbonding onto the enolate moiety due to competition with the π-acidic vinylidene ligand; see later.

(26) Pregosin and co-workers have convincingly demonstrated the ubiquity of "supplemental stabilization", via σ- or π-donation from aromatic sites, of coordinatively unsaturated metal centers bearing atropisomeric phosphine ligands such as BINAP, MOP, and MeO-BIPHEP, as well as some phosphoramidites. See: (a) Pregosin, P. S. *Chem. Commun.* **2008**, 4875–4884. (b) Pregosin, P. S. *Coord. Chem. Rev.* **2008**, *252*, 2156–2170.

(27) The prime label on these carbon nuclei differentiates the two naphthol rings within unsymmetrical complexes: in η^1,η^1-bound complexes such as **3a**/**3b**, it is arbitrary, but in variable-hapticity BINO complexes, specifically, it designates the ring of lower hapticity.

(28) Bruce, M. I. *Chem. Rev.* **1998**, *98*, 2797–2858.

(29) We note that the solid-state structure of **7″** reveals π-stacking interactions between the BINO and the PPh_3 phenyl rings, as well as between the phenyl rings themselves: if these interactions are retained in solution, the resulting ring currents could affect the locations of the aromatic signals (see: Rathore, R.; Abdelwahed, S. H.; Guzei, I. A. *J. Am. Chem. Soc.* **2003**, *125*, 8712–8713), limiting the diagnostic value of the BINO chemical shifts. ^1H and ^{13}C NMR resonances for the phenyl nuclei in **7″** appear within their usual chemical shift ranges, however, suggesting that π-stacking is lost in solution, or has minimal influence. While further examples of the unique η^3,η^3-BINO coordination mode will clarify the issue, we are thus inclined to view the NMR shifts for the BINO ligand in **7″** as arising from the metal−ligand interaction, with a corresponding diagnostic value.

(30) Hallman, P. S.; Stephenson, T. A.; Wilkinson, G. *Inorg. Synth.* **1970**, *12*, 237–40.

(31) Galvan-Arzate, S.; Santamaria, A. *Toxicol. Lett.* **1998**, *99*, 1–13.

(32) The majority of BINO signals can be located for complexes **7′**, **7″**, **9**, **10**, **11**, **12**, and **13**. Full assignment of all $^{13}C\{^1H\}$ NMR peaks is

complicated by the large number of aromatic signals (these account for all resonances, with the exception of the singlets for MeCN in **9** and **10**, and the vinylidene group in **13**), and the simultaneous presence of two species in solution for **7′/7″**, **9/10**, and **11/12**. Unassigned ^{1}H NMR signals for BINO, py, and/or PPh_3 protons are designated as Ar or Ph.

(33) Beurskens, P. T.; Beurskens, G.; de Gelder, R.; Smits, J. M. M.; Garcia-Granda, S.; Gould, R. O. *The DIRDIF-2008 Program System*; Crystallography Laboratory, Radboud University: Nijmegen, The Netherlands, 2008.

(34) Sheldrick, G. M. *Acta Crystallogr.* **2008**, *A64*, 112–122.